

Deconvolution of Kelvin probe force microscopy measurements—methodology and application

T Machleidt, E Sparrer, D Kapusi and K-H Franke

Department of Computer Graphics Program, Ilmenau University of Technology, PO Box 100 565, D-98684 Ilmenau, Germany

E-mail: torsten.machleidt@tu-ilmenau.de

Received 27 November 2008, in final form 1 May 2009

Published 30 June 2009

Online at stacks.iop.org/MST/20/084017

Abstract

Kelvin probe force microscopy (KPFM) is a method to detect the surface potential of micro- and nanostructured samples using a common atomic force microscope (AFM). The electrostatic force has a very long range compared to other surface forces. By using AFM systems under ambient conditions, KPFM measurements are performed using a non-contact regime at surface distances greater than 10 nm. This paper deals with a method to deconvolve the measured KPFM data with the objective to increase the lateral resolution. The KPFM signal is a convolution of an effective surface potential and a microscopic intrinsic point spread function, which allows the restoration of the measured data by linear deconvolution. In contrast to other papers [4], we have developed a new method to use the measured AFM tip shape as a basis to construct the point spread function. The linear shift-invariant channel is introduced as a signal formation model and a Wiener-supported deconvolution algorithm is applied to the measured data. The new method was demonstrated on a nanoscale test stripe pattern for lateral resolution and calibration of length scales (BAM-L200) manufactured by the Federal Institute for Materials Research and Testing, Germany. For the first time, a two-dimensional deconvolution of the KPFM data was able to be demonstrated. An increase in the lateral resolution compared to Strassburg *et al* (2005 *Rev. Sci. Instrum.* **76** 083705) was accomplished. The results demonstrate the necessity of deconvolving the virtually topography-free probe data under ambient conditions.

Keywords: Kelvin probe force microscopy, scanning probe microscopy, deconvolution, point spread function, lateral resolution

(Some figures in this article are in colour only in the electronic version)

1. Introduction

This paper presents investigations of the special atomic force microscope (AFM) mode used in Kelvin probe force microscopy (KPFM). Glatzel [2] estimated that the KPFM resolution is limited. Because common atomic force microscopes are capable of a higher resolution, the measured data seem blurred.

The theory of KPFM is explained in a concise and clear manner by the research group under Rosenwaks and Strassburg [2, 4] and in [3] especially for KPFM on semiconductors.

In [4], Strassburg *et al* explores the possibility of using the deconvolution of KPFM data (UHV). They describe a way to determine the point spread function (PSF) as well as show simulations for determining factors that influence the PSF. The necessity for this is demonstrated using the example of an atomic step on GaP(1 1 0).

This paper presents a new approach to determining the PSF involving the direct integration of the measured tip shape. Using this, a possibility of calculating an asymmetrical PSF with a dependence on the actual tip exists for the first time. This method forms the basis of two-dimensional deconvolution of

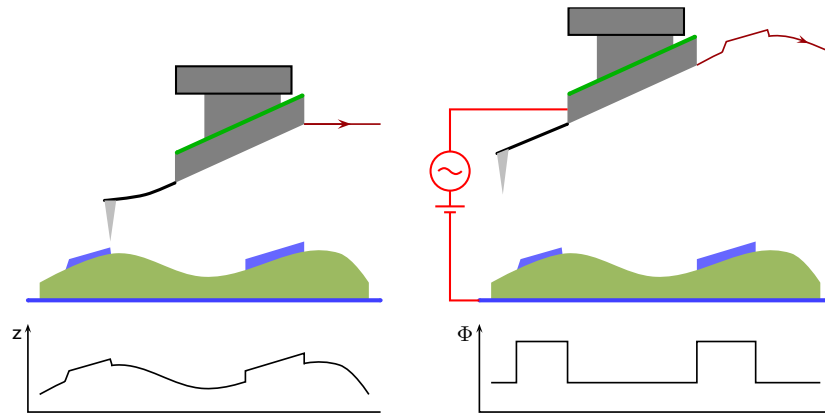


Figure 1. Operating regime of KPFM in two passes. Left: determination of the sample topography. Right: measurement of the surface potential with constant altitude h .

the data. This process was carried out on a certified reference structure with the goal of increasing the lateral resolution. For the first time, a virtually topography-free structure was able to be deconvolved. At the same time, new challenges arose from the further development of the deconvolution method. The results show significant advancements in the deconvolution of KPFM data as compared to the work in [4], but they also underline the necessity for continuing the treatment of the problem.

2. Imaging model of the Kelvin probe force microscopy

Our investigations were done by using a signal formation process to enable the restoration of KPFM data, generated with AFM techniques under ambient conditions. This process is able to enhance the lateral resolution by a factor of 4. KPFM is a method to detect the surface potential of micro- and nanostructured samples using a common atomic force microscope. To detect the surface potential, all surface forces besides the electrostatic force must be eliminated. Because the electrostatic force has a very long range compared to other surface forces, these forces can be eliminated by moving the cantilever tip to a height h of at least 10 nm above the sample surface. Owing to the indirect dependence of the measured electrostatic force on the quadratic distance of the charged objects, this distance must be kept constant for proper measurements. Therefore, a KPFM measurement is done in two passes as shown in figure 1.

In the first pass, the surface topography is detected by applying a commercially available AFM method. To provide a constant altitude h between the tip and surface in the second pass, the cantilever is kept at the desired distance h along the detected surface trajectory. During the measurement, the cantilever is oscillated by applying a voltage U_{ac} between the cantilever and the sample surface, which is modulated at the resonance frequency f_0 of the cantilever. According to Jacobs *et al* [5], when in resonance the acting electrostatic force at the cantilever tip can be expressed by

$$F_{C,\omega_0} = \frac{dC}{dz} \cdot (U_{dc} - \Phi(x, y)) \cdot U_{ac} \cdot \sin(2\pi f_0 t). \quad (1)$$

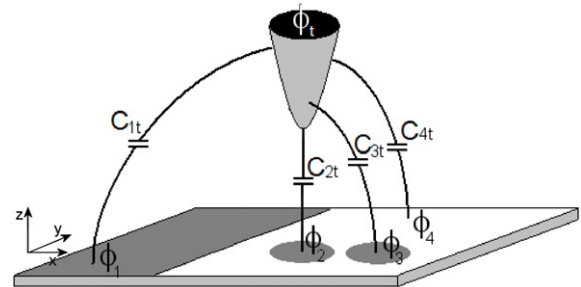


Figure 2. Model of distributed capacitances between the tip and sample surface.

The control system of the KPFM device adjusts an additional direct voltage U_{dc} so that the acting force vanishes as described by equation (2):

$$0 = C'(x, y) \cdot (U_{dc} - \Phi(x, y)) \cdot U_{ac} \cdot \sin(2\pi f_0 t),$$

$$\text{with } C'(x, y) = \frac{dC}{dz}. \quad (2)$$

The absolute value of the measured potential $\Phi_{dc} = U_{dc}$ is equal to the surface potential Φ at the measurement point. The tip to surface capacitance C can be described as a distributed capacitance as depicted in figure 2 and equation (3):

$$C(x, y) = \int_i \int_j C_{ij}(x - x_i, y - y_j) di dj. \quad (3)$$

Equation (2), when solved for the measured potential Φ_{dc} and with the capacitance substituted by equation (3), results in the linear convolution integral given in equation (4):

$$\Phi_{dc}(x, y) = \int_i \int_j \frac{C'_{ij}(x - x_i, y - y_j)}{C'(x, y)} \cdot \Phi(x - x_i, y - y_j) di dj. \quad (4)$$

The fraction described by the distributed capacitance derivations C'_{ij}/C' can be realized as the tip-dependent PSF of the KPFM system. Proving the linear dependence of the measured signal ϕ_{dc} on the actual surface potential ϕ , the linear shift-invariant channel can be introduced as a model to describe the signal formation process [6]. The imaging

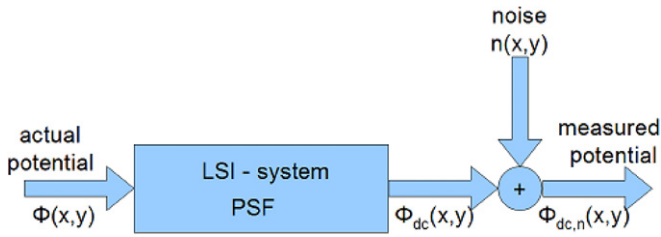


Figure 3. Linear shift-invariant channel.

process for KPFM must be expanded to include an additive noise component. Figure 3 shows the new image generation model for KPFM measurements.

$$\Phi_{dc} = \text{PSF} * \Phi + n, \quad \text{where } * \text{ denotes convolution.} \quad (5)$$

This model allows the restoration of the KPFM data using linear deconvolution:

$$\Phi = \text{PSF}^{-1} * (\Phi_{dc} - n). \quad (6)$$

To deconvolve the data, the PSF of the KPFM system must be known along with a description of the noise in the system. Therefore, a deduction based on the physical interrelations has been applied.

3. Estimation of the PSF of the KPFM system

A method of calculating the electric field based on a prolate spheroidal coordinate system is presented in [7]. Using this coordinate system allows us to determine a straightforward description of the electrostatic field between the charged tip and its mirror charge [8]. According to Gómez-Mónivas *et al* [9], only the apex of the KPFM tip is responsible for the shape of the PSF and the apex can be approximated well by a hyperboloid. The apex shape can be estimated by measuring it using suitable standards, such as (NT-MDT) TGT1 (see figure 4) [10].

The PSF can be derived by transforming the apex surface to polar coordinates and fitting a hyperbola for every angle α .

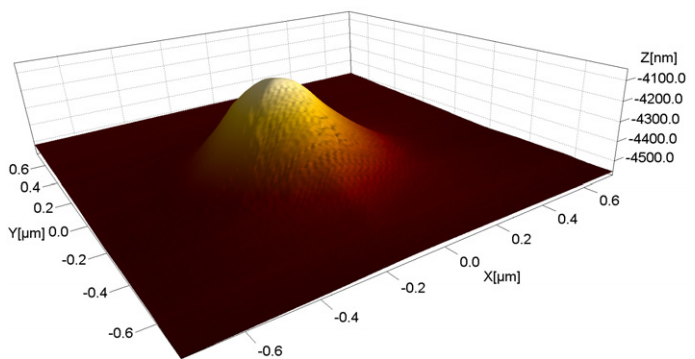
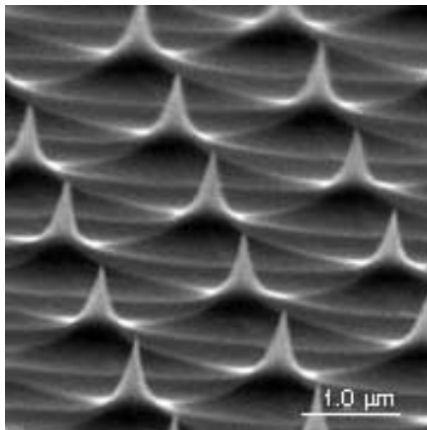


Figure 4. SEM image of standard TGT1 (left) and measurement results achieved by scanning TGT1, which represents the AFM tip shape (right).

The equipotential lines ξ and the field lines η are calculated using the notation in [14] to transform the hyperbola into the prolate spheroidal coordinate system:

$$\begin{aligned} x &= a\sqrt{(\xi^2 - 1)(1 - \eta^2)} \cos \alpha, \\ y &= a\sqrt{(\xi^2 - 1)(1 - \eta^2)} \sin \alpha, \quad z = a\xi\eta. \end{aligned} \quad (7)$$

Similarly, the transformation of Cartesian coordinates into the prolate spheroidal coordinate system is done using the following equation:

$$\begin{aligned} \xi &= \frac{r_1 + r_2}{2a}, \quad \eta = \frac{r_1 - r_2}{2a}, \\ \alpha &= \frac{x}{y}, \quad \text{with } r_{1,2} = \sqrt{(z \pm a)^2 + x^2 + y^2}. \end{aligned} \quad (8)$$

Parameter a describes the distance between the focal point of the hyperbola and the origin. According to [7, 16], the maximum field strength occurs at the tip apex ($\xi = 1, \eta = \eta_s$). In contrast to all other authors, the hyperbola was fitted to the measured tip in slices at angle α . For the first time, the direct form of the probe tip is used to calculate the PSF. For every angle α , the parameters η_s and ξ can be calculated from the parameters of the hyperbola:

$$P^2 = C_1(\alpha)z + C_2(\alpha)z^2 \quad (9)$$

$$\eta_s(\alpha) = \sqrt{\frac{1}{1 + C_2(\alpha)}}, \quad a = \frac{C_1(\alpha)}{2C_2(\alpha)\eta_s}. \quad (10)$$

Using the parameters η_s, ξ which is the electrostatic force acting between a planar surface and the tip apex is given by equation (11). η describes the equipotential lines, η_s the equipotential line at the tip apex's surface and Q the total charge at the tip surface:

$$F_{el}(h, \alpha) = Q \cdot \frac{2\eta_s(\alpha)}{\ln\left(\frac{1+\eta_s(\alpha)}{1-\eta_s(\alpha)}\right)\sqrt{(\xi^2(\alpha) - \eta^2(\alpha))(1 - \eta^2(\alpha))}} \frac{U_{dc}}{h}. \quad (11)$$

Finally, the PSF can be calculated from (11) using a normalizing equation through integration. PSF estimations

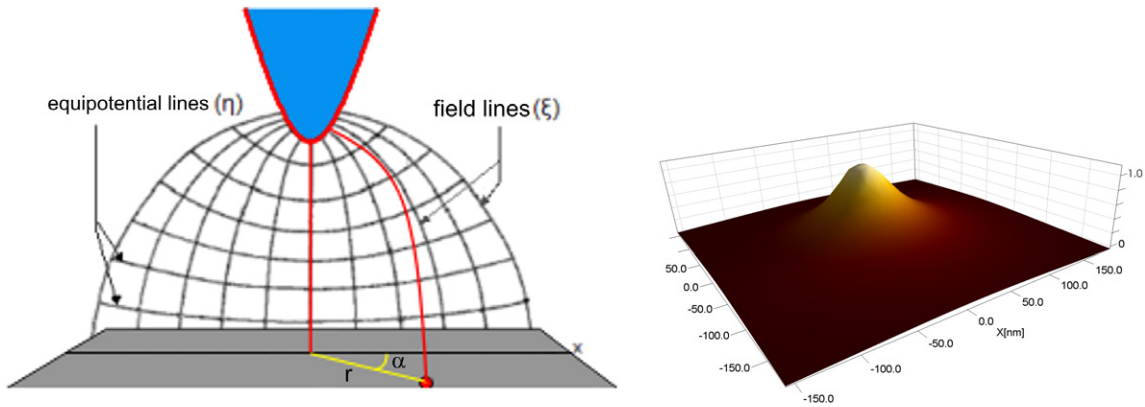


Figure 5. Fitting a hyperbola for every angle α (left) and the calculated PSF (right).

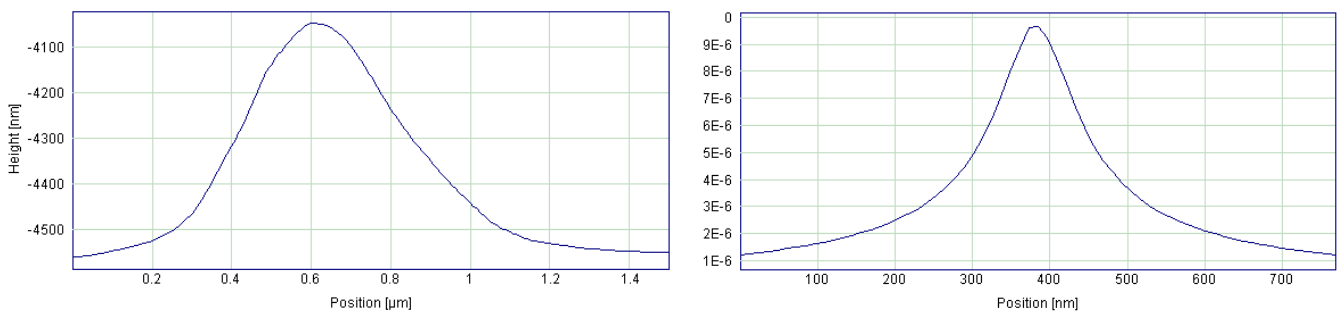


Figure 6. X-profile across the apex of the AFM tip shape (left) and the x-profile across the apex of the calculated PSF (right).

obtained by this method are shown at the right of figure 5. Figure 6 shows the profile of the measured tip shape and the calculated PSF.

4. Deconvolution results

This section presents a demonstration of the deconvolution process. A reconstructed image can be generated using the calculated PSF, the measured data and information about the noise. The noise was determined to be white noise through the analysis of a Fourier-transformed KPFM image. A direct PSF inversion (6) is used to deconvolve the KPFM measurement data. Because the noise is disproportionately amplified at high spatial frequencies by direct deconvolution, the process must be combined with an optimized filter (Wiener filter [15]). The deconvolution can be easily described in the frequency domain by

$$\Phi(f) = \frac{1}{\text{PSF}(f)} \left[\frac{|\text{PSF}(f)|^2}{|\text{PSF}(f)|^2 + \frac{1}{\text{SNR}(f)}} \right] \Phi_{\text{dc}}(f), \quad (12)$$

where $\text{SNR}(f) = \frac{S(f)}{N(f)}$ is the signal-to-noise ratio with $S(f)$ as the mean power spectral density of Φ_{dc} and $N(f)$ as the mean power spectral density of the noise n .

To demonstrate the results, a nanoscale strip pattern BAM-L200 produced by the Federal Institute for Materials Research and Testing in Germany [11] is measured in order to determine the lateral resolution and to calibrate the length scale. The sample has several advantages: it possesses a high material

contrast and has a topography height lower than 10 nm. The structural layout of the sample is shown in figure 7(a).

An AFM of type Atos Solver Pro (NT-MDT) was used under ambient conditions. The measurements were performed using the two-pass technique shown in figure 1 with a TiN tip (NSG10/TiN, NT-MDT, tip curvature radius 35 nm, cone angle $<22^\circ$) and a sample distance h of 100 nm during the second pass. The scan speed was $10 \mu\text{m s}^{-1}$ and the bias in pass 2 was 3 V. Figures 7(b) and (c) give the topographical measurement results and the KPFM results, respectively. The blurring of the KPFM data is clearly evident. The results of applying the deconvolution process described above to restore KPFM data are shown in figure 7(d).

Figure 7(e) shows the topographical profile as well as the raw and the reconstructed KPFM data for better analysis. The original KPFM data (profile 2) are characterized by heavily blurred areas and no detailed structure information. The lateral resolution is larger than 100 nm. In contrast to the measured results, the reconstructed KPFM data (profile 3) show better contrast and a higher lateral resolution of less than 30 nm. This shows an increase in the lateral resolution of a certified reference structure for the first time. Most significant is the two-dimensional application of the deconvolution process, which only yields meaningful results using a PSF of the measured tip shape. Even though the results in figure 7(e) are good, the data in the figure exhibit reconstruction artifacts typical for Wiener deconvolution. They occur due to effects not contained within the model, for example line jumps in the measurement data arising from piezo-like behavior in the

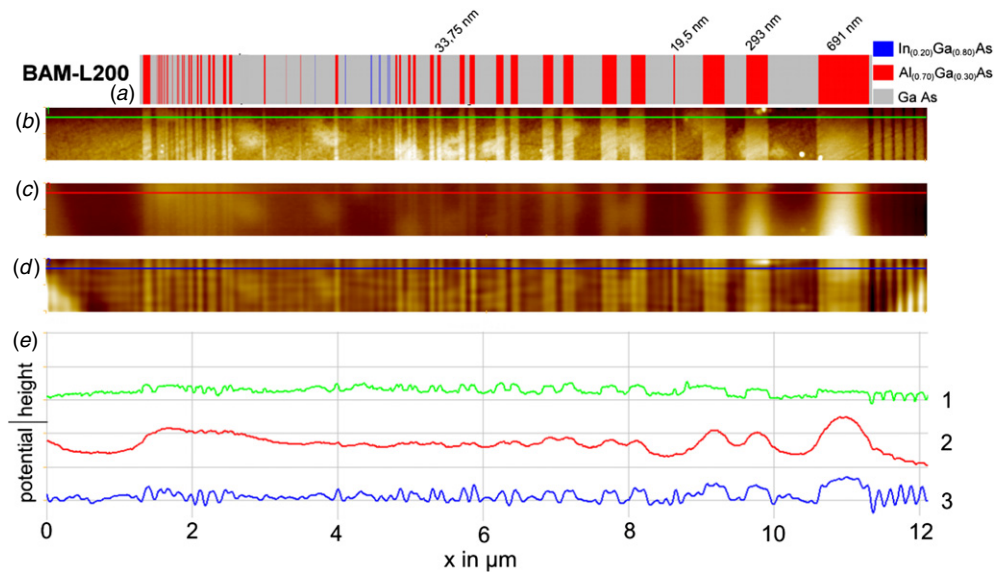


Figure 7. Practical results. (a) Illustration of the BAM-L200 standard, (b) topography measurement, (c) KPFM measurement, (d) deconvolution of the KPFM data, (e) profile of the results ((1) topography, (2) KPFM data, (3) deconvolved KPFM data).

system. The reason for these line jumps is creeping of the piezo as well as small and stochastic low frequency fluctuations of the surface-potential-equivalent dc voltage arising from the principle of measurement.

5. Conclusion and outlook

Assuming that the surface of a sample is a plane, the measured KPFM data can be understood as a convolution of the microscope's inherent transfer function with the actual potential distribution on the sample surface. Therefore, the linear shift-invariant channel can be introduced as a model to describe the signal formation process. By analyzing the physical interrelations, the transfer function can be determined and the measured KPFM data can be deconvolved. The restoration can be achieved by a direct inversion of the transfer function supported by a Wiener filter denoising approach. The deconvolved data allow a better interpretation of the actual potential distribution.

The advantage of the method demonstrated is the use of AFM systems under ambient conditions to measure the sample potential with a lateral resolution lower than 30 nm using the deconvolution process. A critical factor is that some artefacts arise in the restored image. These stem from random artefacts in the measuring process which are not taken into account in the model. In order to solve this problem, a better AFM system or a more complex restoration algorithm must be used. The latter method is demonstrated in [13]. A complex restoration algorithm called the 'pixonen method' was tested in that work. The results are promising, but the elapsed time during the deconvolution of a KPFM image of 100×100 pixels is (at 10 min) more than a factor of 600 slower than the algorithm demonstrated here. In combination with a complex parameterization, this interesting method cannot be used in practice today. Currently, our work is concentrated on implementing the complex restoration algorithm in a graphics

processing unit (GPU). Using the parallel structure of the latest graphics devices should enable us to speed up the restoration process, allowing more and wider practical uses in the future.

Acknowledgments

This work was supported by the German Science Foundation (DFG, SFB 622). The authors wish to thank all those colleagues at the Ilmenau University of Technology and the ZBS Ilmenau eV who contributed to these developments.

References

- [1] Arden W, Cogeze P, Ishiuchi H, Osada T and Moon J T 2006 *International Technology Roadmap For Semiconductors 2006 Update—Overview and Working Group Summaries* <http://www.itrs.net/Links/2006Update/2006UpdateFinal.htm>
- [2] Glatzel Th, Lux-Steiner M Ch, Strassburg E, Boag A and Rosenwaks Y 2007 Principles of Kelvin probe force microscopy *Scanning Probe Microscopy* vol 1 (Berlin: Springer) pp 113–31
- [3] Rosenwaks Y, Saraf S, Tal O, Glatzel Th, Lux-Steiner M Ch, Strassburg E and Boag A 2007 Principles of Kelvin probe force microscopy *Scanning Probe Microscopy* vol 2 (Berlin: Springer) pp 663–89
- [4] Strassburg E, Boag A and Rosenwaks Y 2005 Reconstruction of electrostatic force microscopy images *Rev. Sci. Instrum.* **76** 083705
- [5] Jacobs H O, Leuchtmann P, Homan O J and Stemmer A 1998 *J. Appl. Phys.* **84** 1168–73
- [6] Haykin S 2001 *Communication Systems* 4th edn (New York: Wiley)
- [7] König R 1997 Nanostrukturierung mit dem Rastertunnelmikroskop *Dissertation* TU Braunschweig
- [8] Jackson J D 1999 *Classical Electrodynamics* (Samizdat Press)
- [9] Gómez-Moñivas S, Froufe L S, Carminati R, Greffet J J and Sáenz J J 2001 *Nanotechnology* **12** 496–9
- [10] Machleidt T, Kaestner R and Franke K-H 2005 Reconstruction and geometric assessment of AFM tips *Nanoscale Calibration Standards and Methods* (New York: Wiley) pp 297–310

- [11] Senoner M, Wirth Th, Unger W, Oesterle W, Kaiander I, Sellin R L and Bimberg D 2005 Testing the lateral resolution in the nanometre range with a new type of certified reference material *Nanoscale Calibration Standards and Methods* (New York: Wiley) pp 282–94
- [12] Sparrer E, Nestler R, Machleidt T, Franke K-H and Niebelschütz M 2007 *Proc. 52nd Int. Wissenschaftliches Kolloquium* vol 2 (Ilmenau: TU Ilmenau) pp 245–50
- [13] Nestler R, Machleidt T, Sparrer E and Franke K-H 2008 *Tech. Mess.* **10** 547–54
- [14] Russel A M 1962 *J. Appl. Phys.* **33** 970
- [15] Wiener N 1949 *The Extrapolation, Interpolation, and Smoothing of Stationary Time Series with Engineering Applications* (New York: Wiley)
- [16] Moon P and Spencer D E 1971 *Field Theory Handbook* (Berlin: Springer)